



Evaluation of a solar membrane distillator hybridized with a photovoltaic cell

Kazuo Murase*, Kouki Chikamatsu, Takayuki Kyuno

Chuo University, 1-13-27, Kasuga, Bunkyo-ku, Tokyo, Japan

Tel. +81 (3)3817 1912; Fax: +81 (3)3817 1895; email: hmurase@kc.chuo-u.ac.jp

Received 28 February 2012; Accepted 10 May 2012

ABSTRACT

Solar energy is one of the most promising natural and renewable energy resources. Hybridization is one of the most available concepts that serve as a solution for small-energy conversion of the renewable energy. A hybrid solar membrane distillator with a photovoltaic cell was devised to simultaneously utilize both solar photovoltaic energy and thermal energy. A PV/T system, which has combined a solar cell and a thermal unit for heating or cooling device is one of the hybrid systems. The effectivity of a hybrid solar membrane distillator was experimentally and numerically verified by the case studies of a solar cell, membrane solar distillator with and without a photovoltaic cell. The standard electrical conversion efficiency of a hybrid distillator had equivalent performance as a solar cell without a distillator due to an amorphous Si photovoltaic cell. The reduction of thermal efficiency by hybridization is settled within the 10% range in spite of a larger heat resistance of the hybrid distillator. The performance of a hybrid system of electricity and heat was estimated not by the concept of total system but by the energy-saving efficiency. The energy-saving efficiency of a hybrid distillator, 33%, is obtained beyond our expectations.

Keywords: Hybrid solar distillator; Solar cell; Membrane distillation; PTFE membrane

1. Introduction

Water and energy are indispensable for human life and our industry. However, arid regions and the demand for water sources have been expanding year by year in the world with rapid growth in industrialization. Consumption of natural resources, particularly fossil fuel, for generating huge energy gives rise to a host of environmental problems such as global warming. Therefore, we should effectively tap inexhaustible natural resources such as ocean for water and solar energy as one of the renewable energies. The utiliza-

tion of renewable energy for desalination is one of the most promising technologies to simultaneously resolve both energy and water problems and for the soft global process as reviewed in Ref. [1].

Desalination is one of the chemical separation processes that remove salt from seawater or saline or brackish water. Practical desalination processes are classified in to thermal and non-thermal processes. Thermal processes utilize phase-change process, evaporation and condensation, to produce distilled water using multi-stage flash, vapor compression, and solar fill. Non-thermal processes are membrane separation

*Corresponding author.

processes such as reverse osmosis and electrodialysis. Only membrane distillation (MD) is classified into both thermal and membrane processes. MD has the advantages such as high selectivity of separation, lower temperature or pressure operation, and the high-mass transfer rate as reviewed in Ref. [2]. A solar-driven MD is suitable for a combination of the desalination process and the utilization of renewable energy [3].

On the other hand, solar energy is one of the most promising and all-range renewable energies according to the rapid and diverse development of a solar cell. However, the maximum conversion efficiency of a cell is below it most 35% despite active research conducted on the new type of a solar cell. The low efficiency of a cell results from an independent reuse of the solar energy that is the solar ray or the solar heat. Therefore, several hybrid photovoltaic–thermal systems have been studied to improve the conversion efficiency due to the dependence of cell temperature [4] or to recover the waste heat [5–7].

We have been developing a flat type of solar distillator to answer to the environmental global warming problem of by adopting the irrigation method [8,9]. The flat type of a membrane distillator easily combines with other processes an account of supporting the water surface with a membrane. To effectively tap the solar energy from both energy sources, solar ray and heat, a new solar membrane distillator directly hybridized with a solar cell was set up not in conventional desalination process [10] but in a solar distillator unified with a solar cell. A double-glass solar cell manufactured by Kaneka Co. Ltd. and a wide Poly Tera Fluoro Ethylene (PTFE) membrane by Nitto Denko were selected for the direct hybridization. The effectivity of our hybrid solar membrane distillator was experimentally and numerically investigated.

2. Experimental set-up

Fig. 1 schematically shows the cross-section of a flat-type hybrid solar distillator combined with a solar cell. The double-glass solar cell (manufactured by Kaneka Co. Ltd., Amorphous Si, 1.1 cm in thickness, 0.98 m in length, and 0.95 m in width, $V_{OC}=91.8\text{ V}$, $I_{SC}=1.19\text{ A}$, $P_M=60\text{ W}$, $V_{PM}=67.0\text{ V}$, $I_{PM}=0.90$) is placed on a flat-type membrane distillator. The I – V curve Tracer (Eko Instruments, MP-160) was used to investigate the dynamic fundamental characteristics of a cell, the open-circuit voltage, short-circuit current, conversion efficiency, and fill factor (FF) of solar cell. A flat type of membrane distillator composed of a solar absorber of black-colored Polyethylene tele-

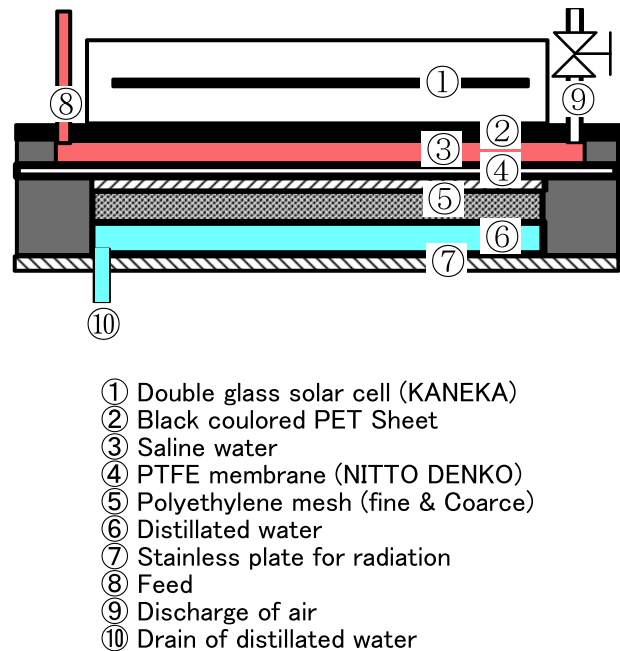


Fig. 1. A schematic cross-section hybrid solar distillator.

phthalate (PET) sheet (1.88 mm in thickness), saline water (2 mm in thickness), PTFE membrane (NITTO-DENKO Co. Ltd., NTF-5200, 1 μm in pore diameter, 85 μm in thickness, and 80% in void fraction), diffusion gap of water vapor supported with fine and coarse types of polyethylene meshes (5 mm in thickness) and radiator of stainless plate (2.2 mm in thickness). The hybrid distillator was tilted at a lower angle, 2°, for a stable water flow and set up at an outdoor situation in JAPAN. The intensity of solar energy was measured with a pyranometer (EKO Instruments Co. Ltd. Model MS-42). Distillate productivity and partition temperatures obtained with copper-constantan thermocouples were, respectively, recorded per one hour and one minute. The volume of water heated through the cell was kept at constant flux. The experimental apparatus was set up on the roof of the four-story building in our University, Tokyo Japan (Latitude 35.7, Longitude 139). Three case studies, standalone PV panel without a membrane distillator, Standalone air gap membrane distillation (AGMD) with a black-colored PET sheet as a solar absorber and a hybrid AGMD, were separately executed in order to estimate the effectivity of hybridization. The photovoltaic performance, particularly conversion efficiency, η , was obtained by the IV curve tracer (EKO Instruments Co. Ltd. Model MP-160) on the basis of experimental data of open-circuit voltage (V_{OC}), short-circuit current (I_{SC}), and maximum power (P_{Max}), FF.

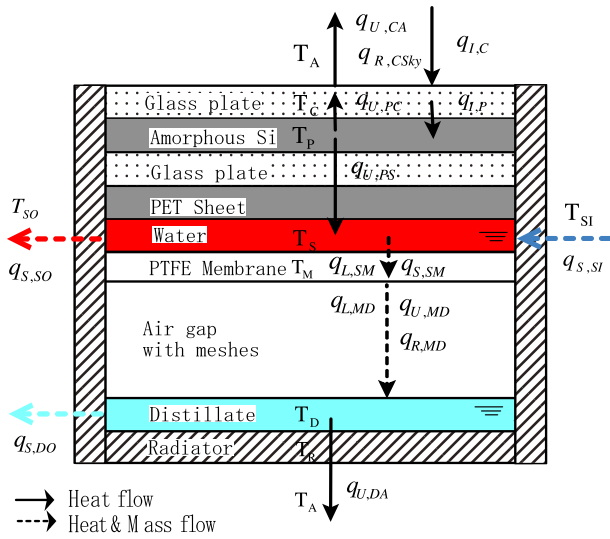


Fig. 2. Heat and mass flow of a hybrid distillator.

3. Numerical simulation

3.1. Heat and mass balances

Fig. 2 shows the flows of heat and mass transfer for the simulation model of a hybrid solar distillator. The said model was constituted on the basis of the following assumptions:

- (1) Temperature gradients in the flow direction are negligible.
- (2) Heat transfers with respect to PET sheet, PTFE membrane, and radiator are approximated as the overall heat transfer coefficients due to only heat conduction.
- (3) Temperature polarization across the PTFE membrane is negligible.
- (4) The mesh spacer within the air gap between the PTFE membrane and the radiator has no effect on the heat and mass transfer.

Energy balances for each partition are presented as follows:

$$\begin{aligned} \text{Glass cover } [T_C] : \rho_C C_{P,C} \ell_C \frac{dT_C}{dt} \\ = q_{I,C} + q_{U,PC} - q_{U,CA} - q_{R,CSky} \end{aligned} \quad (1)$$

$$\begin{aligned} \text{Amorphous Si } [T_P] : \rho_P C_{P,P} \ell_P \frac{dT_P}{dt} \\ = q_{I,P} - q_{U,PC} - q_{U,PS} \end{aligned} \quad (2)$$

$$\begin{aligned} \text{Saline water } [T_S] : \rho_S C_{P,S} \ell_S \left(\frac{dT_S}{dt} + u_S \frac{dT_S}{dx} \right) \\ = q_{U,PS} - q_{S,SM} + q_{S,SI} - q_{S,SO} \end{aligned} \quad (3)$$

$$\begin{aligned} \text{PTFE membrane } [T_M] : \rho_M C_{P,M} \ell_M \frac{dT_M}{dt} \\ = q_{S,SM} - q_{L,MD} - q_{U,MD} \\ - q_{R,MD} \end{aligned} \quad (4)$$

$$\begin{aligned} \text{Distillated water } [T_D] : \rho_D C_{P,D} \ell_D \left(\frac{dT_D}{dt} + u_D \frac{dT_D}{dx} \right) \\ = q_{L,MD} + q_{U,MD} + q_{R,MD} \\ - q_{U,DR} \end{aligned} \quad (5)$$

$$\begin{aligned} \text{Radiator } [T_R] : \\ \rho_R C_{P,R} \ell_R \frac{dT_R}{dt} = q_{U,MR} - q_{U,RA} \end{aligned} \quad (6)$$

The distillate productivity is evaluated using the following expression [11]

$$D = \Gamma \frac{\pi}{RT_{av}} \frac{1}{(\delta/e^{3.6} + z)} \frac{P_S - P_D}{P_{BM}} \quad (7)$$

3.2. Numerical analysis

The heat and mass transfer Eqs. (1)–(7) were numerically simulated by the Runge–Kutta method to estimate the dynamic characteristics for one day and were compared with the experimental data in an open-air situation. Temperature gradients along the flow direction may be negligible due to some partitions with high thermal conductivities. The initial or static conditions were estimated by simulated data at the steady state.

4. Results and discussion

4.1. Performance of a solar cell

4.1.1. Effect of hybridization on the electrical conversion efficiency, $\eta_{\text{electrical}}$

The electrical conversion efficiency of photovoltaic cell, $\eta_{\text{electrical}}$, can be estimated by the following expression using the experimental data, V_{OC} , I_{SC} , I , and FF.

$$\eta_{\text{electrical}} = \frac{P_{\text{Max}}}{I} = \frac{V_{\text{oc}}I_{\text{sc}}FF}{I} \times 100[\%] \quad (8)$$

which FF is defined by $\frac{V_{\text{Max}}I_{\text{Max}}}{V_{\text{oc}}I_{\text{sc}}}$. On the other hand, the effect of cell temperature on the conversion efficiency has been generally presented for several Si cells. Then conversion efficiency, $\eta_{\text{electrical,stan}}$, at the standard condition of solar irradiation, 1 kW/m^2 , and of cell temperature, 25°C , is generally available for the public evaluation due to the free dependency of cell temperature.

Fig. 3 shows one of the time-elapsd profiles of measured and standard conversion efficiency and solar intensity for one day in cases of a solar cell and a hybrid cell. These data were acquired on independent days, 17 July 2011 and 10 August 2011. Drastic drop in the solar intensity depends on the shadow effect of a building especially after 16:00.

July in Japan is one of the best months for measurement due to a smooth profile of the solar intensity. The measured conversion efficiency keeps at an almost constant value for one day. On the other hand, the profile of standard conversion efficiency showed a reverse tendency as compared with one of solar intensity. The same value for both efficiencies at 12:00 shows independency from cell temperature, but converted efficiency is effectively evaluated at a comparatively low range of solar intensity. Solar intensity has large fluctuated profiles even if it were Japanese summer season due to cloud or etc. Figures indicate that conversion efficiencies are independent from

panel temperatures and that conversion efficiencies of Amorphous Si cell are suitable at higher temperatures.

Fig. 4 shows the daily conversion efficiencies day to day to estimate the reproducibility with several measurement days using smooth solar intensity profiles. Conversion efficiencies have a constant value for the clear sky in Japanese summer. The constant averaged efficiencies, probably the maximum value for the available solar cell in Table 1, indicate no effect of hybridization on the performance of a solar cell.

The measurement time interval, one minute, is too small for a fluctuating solar radiation in Japan. After the measured data were excluded for drastically increased and decreased values especially with respect to the efficiencies at the low range of solar intensities, the reasonable data were averaged for one day to minimize the fluctuating error.

4.2. Performance of MD

4.2.1. Effect of hybridization on the temperature profiles of each partition

Fig. 5 indicates the temperature profiles of PET absorber, vapor condensed distillate, radiator plate, air and distribution of solar intensity in two cases of membrane distillator with and without a solar panel. Hybrid distillator is equivalent to a distillator with glass cover. The PET temperature in hybrid distillator is higher than that in standalone MD due to the different absorber that is PET sheet or glass plate. Solar thermal energy is sup-

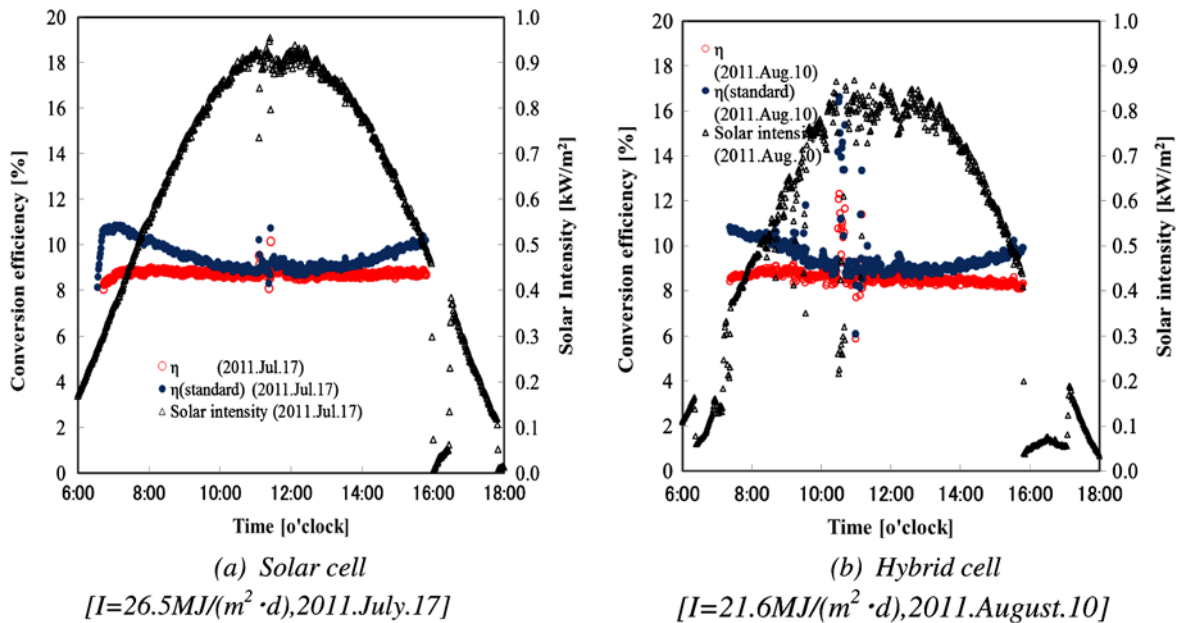


Fig. 3. Profiles of conversion efficiency for one day.

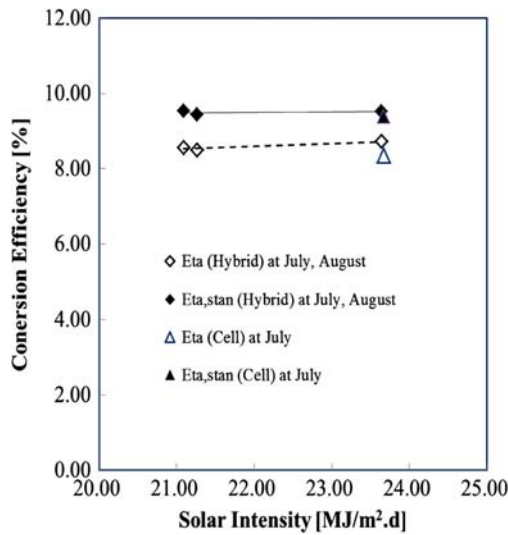


Fig. 4. Daily conversion efficiencies averaged for one month.

posed to be absorbed not in PET sheet but in PV cell of hybrid distillator. Solar cell contributes to higher

temperature of PET but increases heat capacity and heat transfer resistance at PET absorber.

4.2.2. Effect of hybridization on profiles of hourly distillate productivity

Fig. 6 shows the profiles of hourly distillate productivity in two cases of hybrid distillator (Hybrid) and membrane distillator without a photovoltaic cell (AGMD). Profiles of distillate productivity are coordinately recognized. Standalone MD produces the more distillate with the less solar intensity compared with hybrid distillator due to the less heat capacity. The effect of heat accumulation within both devices was scarcely expected due to the slight time lag between distillate productivity and solar intensity.

4.2.3. Effect of hybridization on distillate productivity

The thermal efficiency of a distillator, $\eta_{thermal}$, can be estimated by the following expression for distillate productivity.

Table 1
Averaged conversion efficiency in Fig. 4

	Solar intensity [MJ]/(m ² d)	Efficiency $\eta_{electrical}$ [%]	Standard Efficiency $\eta_{electrical,stan.}$ [%]
(a) Solar cell (July 2011)	25.4	8.56	9.58
(b) Hybrid distillator (August 2011)	22.0	8.60	9.50

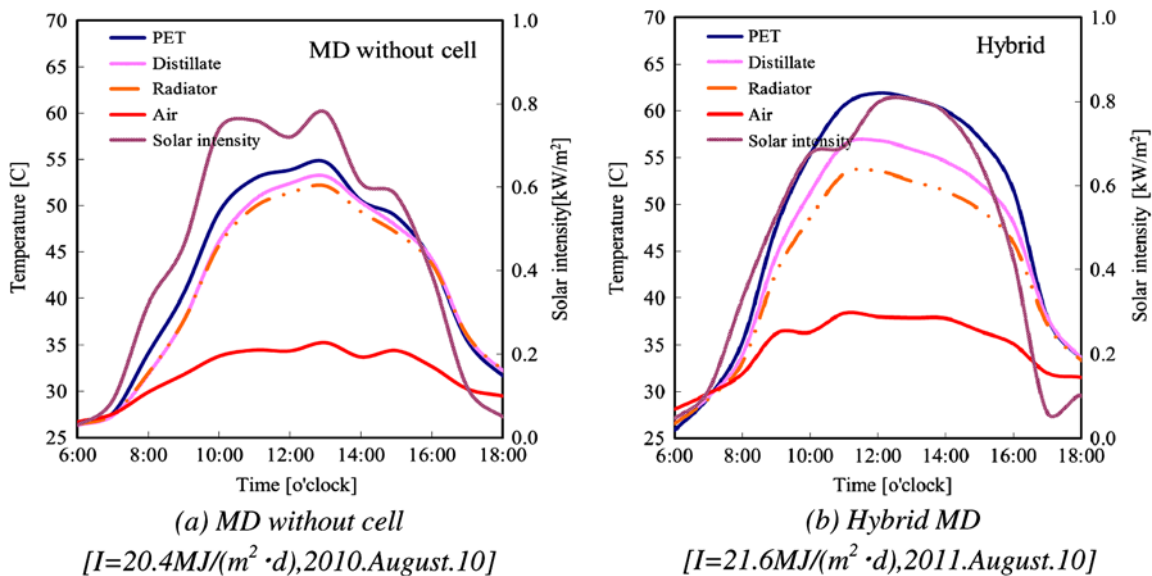


Fig. 5. Effect of hybridization on the temperature profiles of each partition.

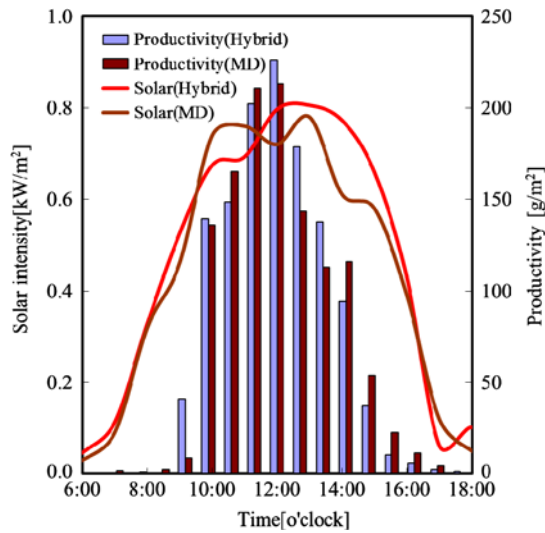


Fig. 6. Effect of hybridization on the profiles of hourly distillate productivity.

$$\eta_{\text{thermal}} = \frac{\lambda \sum D_i}{\sum I_i} \times 100[\%], \quad (9)$$

which \sum_i means the summation for one day.

Fig. 7 show the effect of daily solar intensity on daily distillate productivity and thermal efficiency by

Eq. (9). These markers in Fig. 7 were classified by month. The maximum solar intensity was measured not in August but in July due to the stable solar radiation. The comparison between Fig. 7(a) and (b) indicates that the maximum solar intensity did not always contribute to the maximum thermal efficiency. The maximum thermal efficiency was obtained on the wide range of conditions of solar intensity, which accumulates the solar heat within a distillator. Fluctuating solar radiation did not contribute to thermal efficiency. The experimental data were drastically reduced even during the summer season in Japan due to less solar intensity than in the other arid lands.

Two experimental data in Fig. 7 were selected for evaluating the effectivity of hybridization due to the almost same daily solar intensity. Total distillate productivity and thermal efficiency were list up in Table 2. In spite of the larger heat resistance of hybrid distillator thermal efficiency was reduced within 9.7% as compared with AGMD.

4.2.4. Numerical results

Fig. 8 show the profiles of dynamic distillate productivity by the numerical simulation in two cases of a membrane distillator with and without a photo-

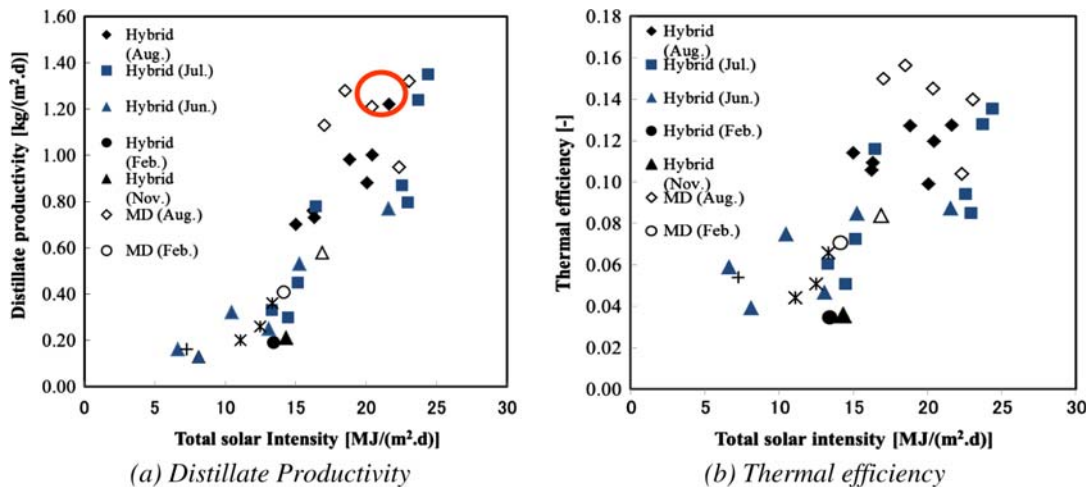


Fig. 7. Effect of solar intensity on distillate productivity.

Table 2
Total distillate productivity per a day in the cases of MD with and without a cell

	Solar intensity [MJ]/(m ² .d)]	Distillate productivity [kg/(m ² .d)]	Thermal efficiency η_{thermal} [%]
(1) AGMD (11 August 2010)	20.4	1.21	14.5
(2) Hybrid (10 August 2010)	21.6	1.22	12.7

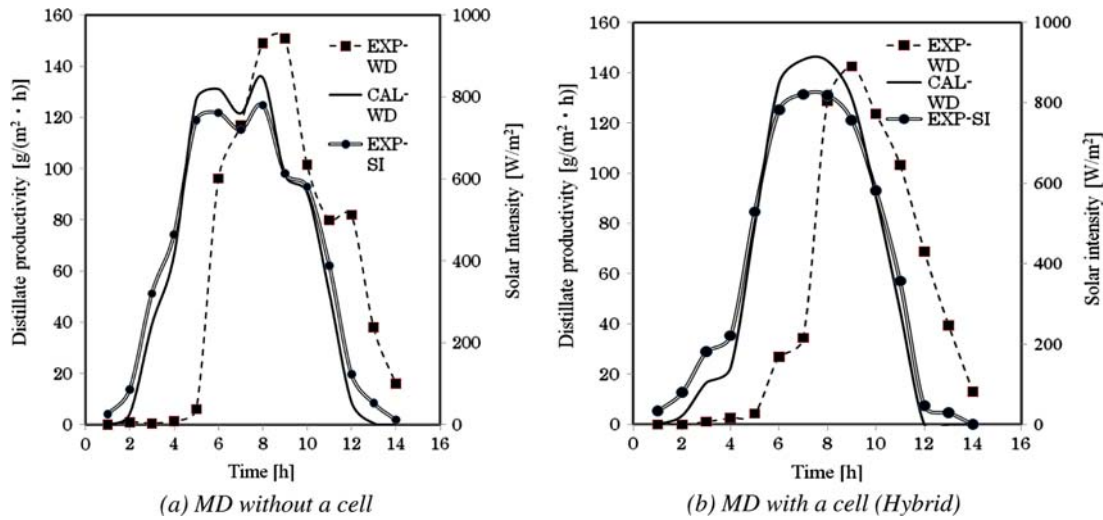


Fig. 8. Numerical prediction of distillate productivity.

Table 3
System performance for solar cell, AGMD, and hybrid distillator

	Solar intensity [MJ]/(m ² d)	Electrical efficiency $\eta_{\text{electrical}}$ [%]	Solar intensity [MJ]/(m ² d)	Thermal Efficiency η_{thermal} [%]	Saving Efficiency η_{saving} [%]
(1) Solar cell	25.4	9.58			25.2
(2) AGMD			23.1	9.3	9.3
(3) Hybrid distillator	22.0	9.50	20.4	8.4	33.4

voltaic cell. The experimental solar intensity and air temperature were used as the weather parameters. The peak value of distillate productivity is underestimated as the productivity in Fig. 8(a) was calculated by the hybrid simulation model. Both profiles of productivity in Fig. 8(a) and (b) were accordingly traced by the model. However, experimental times at peak productivity were shifted by two hours from that of solar intensity. The calculated productivity has a response with no time lags for solar intensity due to the negligible temperature gradient along the water flow. The assumption will be invalid in the case of operational conditions of water flow. The larger specific heat of water and the thickness of a spacer mesh than the other partitions result in the time lag.

4.2.5. Performance of overall hybrid system

The most simple performance for a hybrid system is estimated on the concept of total system, which is

presented by the arithmetic summation of electrical and thermal efficiencies by Eq. (10) [12]. On the other hand, the different grade of electrical and thermal

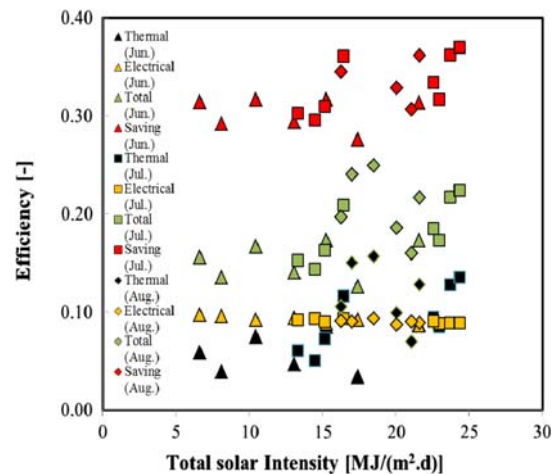


Fig. 9. Effect of daily solar intensity on the various daily efficiencies for each month.

Table 4
Daily efficiencies on hybrid solar distillator averaged for one month

	Solar intensity [MJ]/(m ² d)]	Electrical efficiency $\eta_{\text{electrical}}$ [%]	Solar intensity [MJ]/(m ² d)]	Thermal efficiency η_{thermal} [%]	Saving efficiency η_{saving} [%]
June 2011	13.2	6.1	9.2	15.3	30.3
July 2011	19.1	9.3	9.1	18.3	33.1
August 2011	19.1	11.8	9.0	20.8	33.5

energies should be converted to be equivalent energy grade. Electricity is converted by thermal energy. The energy saving efficiency is described by the summation of thermal energy and electrical energy divided by the electrical energy generation efficiency, which is conventionally set to be the value from 0.3 to 0.4. as Eq. (11) [13]. In this work the efficiency is temporarily fixed to be 0.38. This work adopted for the energy saving efficiency, which is defined by the following expression for distillate productivity.

$$\eta_{\text{total}} = \eta_{\text{thermal}} + \eta_{\text{electrical}} [\%] \quad (10)$$

$$\eta_{\text{saving}} = \eta_{\text{thermal}} + \frac{\eta_{\text{electrical}} [\%]}{\eta_{\text{power}}}, \quad (11)$$

which η_{power} is the electric power generation efficiency of a conventional power plant, which is almost approximated by 0.38. Table 3 indicate the summary of efficiencies for three case study for standalone solar cell, standalone AGMD, and hybrid distillator.

All daily efficiency data, that is thermal, electrical, total system, and energy saving efficiencies, were plotted in Fig. 9. They were averaged for one month. August is the summer season of maximum solar intensity and maximum distillate productivity. The season contributes not to electrical efficiency but to thermal efficiency. The monthly averaged energy saving efficiency of a hybrid membrane distillator was obtained to be more than 30% efficiency at three higher monthly solar intensity.

Table 4 shows the daily efficiencies on hybrid solar distillator averaged for one month in order to estimate the effect of season.

The season contributes not to electrical efficiency but to thermal efficiency. The energy saving efficiency was obtained to be more than 30% even if three monthly solar intensity. The monthly averaged energy saving efficiency of a hybrid membrane distillator was obtained to be more than 30% efficiency at three months.

5. Conclusions

A hybrid solar distillator was devised to simultaneously utilize both solar photovoltaic energy and thermal energy. The effectivity of a solar membrane distillator hybridized with a photovoltaic cell was experimentally and numerically verified by the case studies of a solar cell, membrane solar distillator with and without a photovoltaic cell.

- (1) The large difference in the electrical conversion efficiency between a solar cell and hybrid distillator was hardly recognized due to an amorphous Si PV cell. The constant electrical efficiency is more than 9.0% even if the lower solar intensity.
- (2) The reduction in thermal efficiency by hybridization is settled within the 10% in spite of a larger heat resistance of the hybrid distillator. But the energy saving efficiency of a hybrid MD was increased by four times of thermal efficiency.
- (3) The monthly averaged energy saving efficiency of a hybrid MD was obtained to be more than 30% efficiency at three higher months.
- (4) Electrical efficiency contributes to enhancement of energy saving efficiency due to the higher grade energy of electricity.

Acknowledgements

The work was supported by a grant from the Salt Science Research Foundation (Project No 11A3). Moreover we are grateful for supporting an amorphous-Si solar cell panel by KANEKA Co. Ltd., PTFE membrane by NITTO DENKO Co. Ltd and PET sheet by LINTEC Co. Ltd.

Symbols

C_P	— specific heat, J/(kg K)
D	— distillate productivity, kg/(m ² s)
e	— porosity of the PTFE membrane, –
FF	— fill factor, –
I	— solar intensity, W/m ²
I_{SC}	— short-circuit Current A

k	— thermal conductivity, W/(m K)
l	— thickness of partition, m
L	— length of a hybrid distillator, m
P	— saturated vapor pressure, Pa
P_{Max}	— maximum power, W/m ²
q_I	— heat flux from solar energy, W/m ²
q_L	— latent heat flux, W/m ²
q_R	— radiative heat flux, W/m ²
q_S	— sensitive heat flux, W/m ²
q_U	— overall heat flux, W/m ²
R	— gas constant, Pa m ³ /(mol K)
T	— temperature, K
u	— water velocity, m/s
U	— overall heat transfer coefficient, W/(m ² K)
V_{OC}	— open circuit voltage, V
z	— interval, m

Greeks

α	— absorptivity of partition, —
Γ	— diffusion coefficient of vapor into air, m/s ²
δ	— membrane thickness, m
ε	— emissivity of partition, —
λ	— latent heat of vapor, J/kg
ρ	— density, kg/m ³
σ	— Stefan–Boltzmann constant, W/(m ² K ⁴)
$\eta_{\text{electrical}}$	— electrical conversion efficiency, %
$\eta_{\text{electrical, stan}}$	— standard electrical conversion efficiency, %
η_{power}	— electric power generation efficiency, %
η_{saving}	— energy saving efficiency, %
η_{thermal}	— thermal efficiency, %

References

- [1] S.A. Kalogirou, Seawater desalination using renewable energy sources, *Prog. Energy Combustion Sci.* 31 (2005) 242–281.
- [2] M. Khayet, Membrane and theoretical modeling of membrane distillation: A review, *Adv. Colloid Interface Sci.* 164 (2011) 56–88.
- [3] H. Chang, G.-B. Wang, Y.-H. Chen, C.-C. Li, C.-L. Chang, Modeling and optimization of a solar driven membrane distillation desalination system, *Renewable Energy* 35 (2010) 2714–2722.
- [4] E. Skoplaki, A.G. Boudouvis, J.A. Palyvos, A simple correlation for the operating temperature of photovoltaic modules of arbitrary mounting, *Sol. Energy Mater. Solar Cells* 92 (2008) 1393–1402.
- [5] T.T. Chow, W. He, J. Ji, Hybrid photovoltaic-thermosiphon water heating system for residential application, *Sol. Energy* 80 (2006) 298–306.
- [6] R.M. da Silva, J.L.M. Fernandes, Hybrid photovoltaic/thermal (PV/T) solar systems simulation with Simulink/Matlab, *Sol. Energy* 84 (2010) 1985–1996.
- [7] A. Tiwari, M.S. Sodha, Performance evaluation of hybrid PV/thermal water/air heating system: A parametric study, *Renewable Energy* 31 (2006) 2460–2474.
- [8] K. Murase, S. Komiyama, A. Ikeya, Y. Furukawa, Development of multi-effect membrane solar distillator, *Bull. Soc. Sea Water Sci. Japan* 54 (2000) 30–36.
- [9] K. Murase, Y. Yamagishi, K. Tano, Development of a hybrid solar distillator of a basin type distillator and a membrane distillator, *Desalin. Water Treat.* 9 (2009) 96–104.
- [10] S. Kumar, A. Tiwari, Design, fabrication and performance of a hybrid photovoltaic/thermal (PV/T) active solar still, *Energy Convers. Manage.* 51 (2010) 1219–1229.
- [11] H. Kurokawa, Y. Koseki, A. Yamada, K. Ebara, S. Takahashi, Characteristics of water vapor permeation in membrane distillation, *Kagaku Kogaku Ronbunshu* 14 (1988) 330–336.
- [12] T. Bergene, I.M. Lovvik, Model calculations on a flat-plate solar heat collector with integrated solar cells, *Sol. Energy* 55 (1995) 453–462.
- [13] B.J. Huang, T.H. Lin, W.C. Hung, F.S. Sun, Performance evaluation of solar photovoltaic/thermal systems, *Sol. Energy* 70 (2001) 443–448.